

## Image-guided tissue engineering

Jeffrey J. Ballyns, Lawrence J. Bonassar \*

Cornell University, Biomedical Engineering, Ithaca, NY, USA

Received: November 18, 2008; Accepted: June 16, 2009

- Introduction
- Imaging techniques
- Fabrication techniques
  - Injection moulding
  - Rapid prototyping
  - Lithography
  - Sintering
- Conclusions

### Abstract

Replication of anatomic shape is a significant challenge in developing implants for regenerative medicine. This has led to significant interest in using medical imaging techniques such as magnetic resonance imaging and computed tomography to design tissue engineered constructs. Implementation of medical imaging and computer aided design in combination with technologies for rapid prototyping of living implants enables the generation of highly reproducible constructs with spatial resolution up to 25  $\mu\text{m}$ . In this paper, we review the medical imaging modalities available and a paradigm for choosing a particular imaging technique. We also present fabrication techniques and methodologies for producing cellular engineered constructs. Finally, we comment on future challenges involved with image guided tissue engineering and efforts to generate engineered constructs ready for implantation.

**Keywords:** tissue engineering • image guided • anatomically shaped • scaffolds • injection moulding • rapid prototyping

### Introduction

Tissue engineering attempts to generate new living tissues through the use of engineering principles and biological sciences [1]. There are many different techniques and methodologies used to generate these new tissues (Fig. 1), which have progressed beyond contemporary structural design. Traditionally, when constructing a building, the process begins with the designer using a protractor, straight edge and compass to produce a sketch that will be translated to computer aided design (CAD) software for blueprint production. However, in nature, one rarely sees right angles and straight edges. In the human body the curved surfaces on the exterior of the body result in one's identity (*e.g.* facial mapping and finger prints). Internally, geometric features result in proper joint load distributions in the hip, knee and ankle. Blood flow in a beating heart is properly restricted by the size and behaviour of leaflet valves. Larger organs, such as the liver, have highly organized circulating systems necessary to deliver oxygenated blood through the larger structure. Replicating the complex

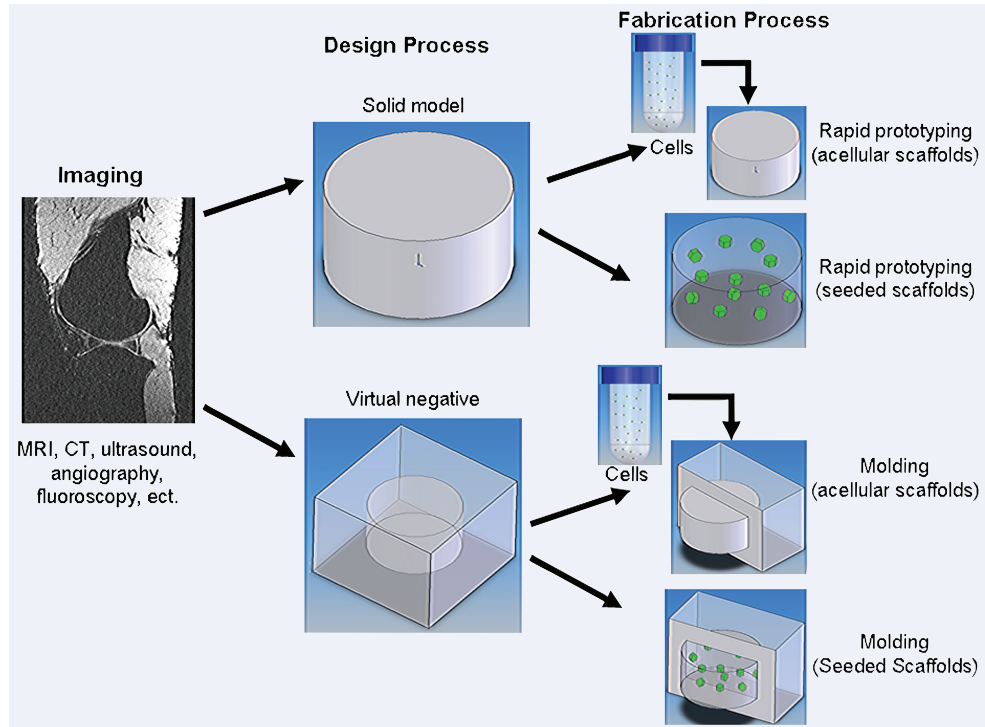
geometries in naturally occurring structures in the body will require more than protractor and compass. To this end, the development of high-resolution imaging techniques combined with bio-materials processing technology has given rise to the field of image-guided tissue engineering.

Typically, imaging modalities such as magnetic resonance imaging (MRI) and computed tomography (CT) have been used as diagnostic tools to visualize the body and develop treatment strategies. Treatment strategies include choosing the type of implant, designing a patient specific implant/prosthetic or perhaps using medical imaging data to guide implantation of a device. Medical imaging can be used not only for prosthetic designs, but can serve as templates for organ scaffold construction. Medically, there exists a large need to provide alternatives for cadaveric allografts, autografts and prosthetic implantations. For example in orthopaedic surgery, the number of patients receiving total hip and knee replacements in 1995 totalled 457,000 in the United States

\*Correspondence to: Lawrence J. BONASSAR,  
Department of Biomedical Engineering,  
Sibley School of Mechanical and Aerospace Engineering,  
Cornell University, 149 Weill Hall,

Ithaca, NY 14853, USA.  
Tel.: (607) 255-9381  
Fax: (607) 255-7730  
E-mail: lb244@cornell.edu

**Fig. 1** Image guided tissue engineering process tree.



alone and is expected to double by the year 2025 [2]. Although the number of patients affected is smaller, those awaiting liver transplant had a death rate of 8.3% in 1999 [3]. Similarly, patients awaiting a heart transplant have a 6-month mortality rate of 24–70% [4]. Facial reconstruction, though less life threatening, represents a cornerstone that interfaces cosmetic and reconstructive surgery to restore both functionality and aesthetic properties important to one's quality of life [5].

Regardless of applications, control of the geometry of transplanted tissue is important. Internally transplanted tissues need to fit into the desired space and conform to the surrounding tissues. As a result, surgeons are often required to manually alter the organs/tissues to 'fit' the recipient whether it is a liver, heart, meniscus, or flap of skin. In addition to function, external tissue transplants require appearance to be taken into consideration as well. However, aesthetic appearance becomes a secondary objective to functionality and restoration of health, because no established treatment exists that meets all other primary criteria to prevent rejection, chronic pain and decrease mortality. Indeed some of the most exciting applications of tissue engineered (TE) technology have involved replication of anatomic geometry.

Some early examples in the field of tissue engineering have been successful in forming cartilage in the shape of a human ear [6], producing a bone-cartilage composite shaped as a mandibular joint [7], generation of a distal phalanx for thumb reconstruction [8] and anatomically shaped menisci for the knee [9]. In these cases, geometry was generated from moulds taken from the

intended tissue. These initial studies, although very important, are unlikely to be implemented on a wide scale for generating patient specific geometry on a case by case basis. An obvious solution would be using medical imaging to obtain the necessary information on the patient's specific anatomical needs. This article will present a brief review of the current methods used to replicate the complex tissues in the body.

## Imaging techniques

Anatomical geometries can be extracted from any medical imaging modality capable of rendering a 3D image, such as angiography, fluoroscopy, mammography, MRI, CT,  $\mu$ CT, stereophotogrammetry (3D photogrammy) and ultrasound. Although there exists a large selection of imaging modalities from which to choose, MRI and CT are the most widely used to visualize cardiovascular, musculoskeletal, neural and dental tissues. However, each imaging technique may present distinct advantages for a specific application of tissue replacement.

MRI can readily register bone and soft tissues and has scan volumes that can range from as large as the human body to small precision scans that image the wrist and knee (Table 1). Scan times for an MRI range from 5 to 40 min. with resolutions that increase with both scan time and magnetic coil strength.

**Table 1** Image modality characteristics

Imaging technique	Preferred tissue	Highest resolution	Scan time	Maximum volume	Safety/compliance
MRI (3T)	Soft tissue and bone	250 $\mu\text{m} \times 250 \mu\text{m} \times 0.5 \text{ mm}$	5–40 min.	Human body	Anxiety/claustrophobia
CT	Bone*	0.24–0.33 mm	5 min. (8–40 sec of actual scan time)	Human body	Ionizing radiation
$\mu\text{CT}$	Bone*	1–200 $\mu\text{m}$	2–4 hrs	Whole rat	Ionizing radiation
Ultrasound	All tissues	1 $\times$ 1.5 $\times$ 0.2 mm	10–15 min.	Blood vessel - neonatal	N/A
3D digital photogrammy	External structures (craniofacial)	150 $\mu\text{m}$	<1 min.	Whole head	N/A

\* = other tissues can be imaged with the aid of contrast agents. Specifications for MRI, CT, and  $\mu\text{CT}$  provided by Siemens Medical Solutions USA, Inc. Malvern, PA, USA and GE Healthcare, formerly EVS Corporation, Ontario, Canada. 3D digital photogrammy specifications provided by 3dMD, Atlanta, GA, USA and ultrasound specifications provided by Elliott and Thrush [12].

Resolutions for a 3T MRI have been reported as high as 250  $\mu\text{m} \times 250 \mu\text{m} \times 0.5 \text{ mm}$ . Scan time can be reduced with the use of higher powered magnetic fields, but human beings are rarely exposed to fields greater than 3 Tesla (T). Exposure to a 7T MR coil can cause higher incidence of discomfort and sensations of vertigo than lower strength MR coils [10]. Although MRI scans are preferred over CT because there is no radiation exposure, it is important to note that there is a sizable percentage of the population that experiences uncomfortable anxiety and claustrophobia when having a full body MRI (Table 1).

CT scans can generate higher resolution images than MRI (0.24–0.33 mm), but can only image bone without the use of contrast agents (Table 1). Three-dimensional models are more readily generated from CT scans with little to no manual editing, whereas MRI requires many manual techniques to acquire the geometry [11]. Scan times are much shorter for CT than for MRI, but this imaging technique requires the use of ionizing radiation. This presents a minimal but finite risk to individual patients, but collectively a much bigger risk to larger patient population.

$\mu\text{CT}$  has ultra high resolution (1–200  $\mu\text{m}$ ), but is limited by the volume in which it can scan (Table 1). Due to the volume limitation of  $\mu\text{CT}$ , it cannot be considered non-invasive for animals larger than mice. Also,  $\mu\text{CT}$ , like CT, will not readily register soft tissues in the absence of contrast agents, which may alter tissue structure or geometry.

Ultrasound can readily image most tissue and does not use ionizing radiation or require a person to be in an enclosed area. Although scan times for ultrasound are short, it is limited in the resolution quality it can provide (1  $\times$  1.5  $\times$  0.2 mm) [12]. Typical volumes that are scanned *via* ultrasound include small structures such as blood vessels to large ones such as neonatal infants (Table 1).

Three-dimensional digital photogrammy can obtain high-resolution images (150  $\mu\text{m}$ ) in less than a minute (Table 1). Three-dimensional photogrammy is primarily used for external

structures it is done in an open area so patients do not have to worry about the claustrophobia that is common to MRI. Further, there is no ionizing radiation associated with 3D digital photogrammy, unlike CT or  $\mu\text{CT}$ .

The process for selecting the most appropriate imaging method is tightly coupled to the target tissue. For example, if the desire is to obtain medical imaging data from a patient to generate a femoral head, meniscus, or heart leaflet valve, three very different approaches would be used. In the case of the femoral head, although CT would provide the highest resolution image of the boney structure, it does not image cartilage or soft tissues readily.  $\mu\text{CT}$  would not be used because the femoral head is too large to fit into current scanning devices. An MRI scan, on the other hand, could be used to obtain both the articular surface and boney structure without contrast agents.

In the case of the meniscus, the most medically relevant choice is MRI. High-resolution images of the meniscus can be obtained *via* MRI by increasing the scan time. However, increased scan time increases cost and becomes a compliancy issue for the patient. The longer the patient is required to remain still during the scan the higher the probability of geometry artefact due to movement. The alternative would be to excise the tissue from the joint, soak it in a contrast agent to allow for  $\mu\text{CT}$  scanning. It is important to note that MRI can acquire geometries under loaded conditions whereas  $\mu\text{CT}$  may have altered geometry due to being soaked in a contrast agent.

In the case of the heart valve, MRI and CT both require contrast agents to visualize the inner workings of the heart and have similar image resolutions. Due to the high radiation exposure needed to perform a CT scan of the heart and the high expense associated with MRI usage, echocardiography (cardiac ultrasound) is becoming a more widely used non-invasive method to obtain 3D geometric models of mitral valves [13, 14]. However, to maximize resolution, the valve can still be excised, soaked in a contrast agent and scanned *via*  $\mu\text{CT}$ .

## Fabrication techniques

Generating anatomically shaped engineered tissues does not require medical images. As mentioned earlier, many early TE efforts to generate anatomically shaped constructs used impression moulds [6, 7, 15–18] to serve as negative templates. The paradigm shift to using medical images for CAD design has only very recently been established [9]. There are multiple methods to replicate anatomical shape through injection moulding or different rapid prototyping techniques and for each method there exists an even larger choice of biomaterials to use as a scaffold. Choice of scaffold will dictate the design and fabrication process of the engineered tissue, which is driven by the application and tissue one is trying to generate. Here we will briefly take a look at some promising results across a number of different engineered tissues.

### Injection moulding

As stated above, scaffold choice has a major role in guiding the fabrication process of generating TE constructs. Many traditional scaffold materials (*e.g.* polyglycolic acid fibres [PGA], polylactic acid [PLA], polycaprolactone [PCL]) require processing at high temperatures or in organic solvents to control shape. As such cells cannot be introduced until the scaffold has cooled and solvents have been removed. In contrast, materials such as hydrogels undergo phase transitions that enable maintenance of cell viability during gel formation. As such, cells can be introduced to these materials prior to moulding.

Initial efforts in cartilage tissue engineering used acellular scaffolds and began with the simple geometries in the shape of triangles, rectangles and cylinders [17]. More complicated geometries were also achieved, such as a human ear using a synthetic non-woven mesh composed of PGA [6]. The PGA mesh was moulded into desired geometries through the use of plaster prosthetic mould, cells were then later seeded onto PGA scaffolds and allowed to culture subcutaneously in nude mice [6, 17].

Similarly, bone TE requires scaffolds with a high rigidity that emulates the physical properties of native bone. The processes involved in bone scaffold formation are often unfavourable for cell viability and therefore seeding of these constructs occurred after they were constructed. One such study successfully TE phalanges and small joints through the use of PGA and PLA [16].

The seeding of acellular scaffolds has also been applied to engineered cardiovascular tissue such as blood vessels and heart valves. In one promising study, PCL was electro-spun into the shape of a trileaflet valve using a custom designed aluminium template modelled after native tissue before being seeded with cardiac cells for *in vitro* culture [19].

Although seeding cells after scaffold generation has produced promising results, this methodology is very time consuming and does not ensure equal cell distribution throughout the scaffold. A more efficient approach would be to seed scaffolds before they are formed, though this would require biomaterials with a non-toxic

liquid phase that maintain viability during the solidification or gelation process. Biomaterials that allow this approach include, but are not limited to, alginate, agarose, chitosan, collagen gel, fibrin glue and poly(lactide-co-glycolide) (PLG). Some of the first such studies involved seeding chondrocytes into alginate [15]. The alginate-cell solution was cross-linked with CaSO<sub>4</sub> and injected into silastic impression moulds of chin and nose implants for facial reconstruction. Using various cell seeding densities they were able to culture these implants in the back of nude mice for 30 weeks and maintain both shape and cell viability [15].

Uniform cell distribution becomes more critical when generating injection moulds of larger constructs, such as the mandible for craniofacial reconstruction [15, 18] or the meniscus of the knee [9]. Seeding the scaffold while it is liquid enhances homogeneity of cell distribution upon initial construct formation. CAD-based injection moulds have been used to design a wide array of geometries from very small volume structures such as tympanic membrane patches (3  $\mu$ l) [20], and engineered heart valves (~1 ml) [21], to larger sized tissues such as the meniscus (2–5 ml) [9]. The resolution for injection moulding has been reported to be 600  $\mu$ m [22].

Injection moulding techniques, although not optimal for multi-material constructs, can be altered to generate more complex tissues. A prime example is the production of an anatomically shaped osteochondral construct based on stereophotogrammetry data *via* injection moulding [23]. Patellar shaped composites were made possible through computer numerical control (CNC) milling of demarrowed bone blocks that fit into a mould allowing for injection of cell seeded agarose resulting in partially integrated bone plugs [23]. Another composite injection moulding study by Mizuno *et al.* produced both a multi-material and multi-cellular TE intervertebral disc [24, 25]. The intervertebral disc was composed of an annulus fibrosus made from PLA/PGA scaffold and a nucleus pulposus made from calcium cross-linked alginate that was injected into the centre void of the PLA/PGA scaffold. Each region was composed of its respective cell type and exhibited both biochemical and mechanical properties similar to that of native tissue [24, 25].

One of the most recent advances in generating patient specific implants *via* injection moulding were achieved using alginate and meniscal fibrochondrocytes from bovine knees [9]. The geometry was obtained using both MRI and  $\mu$ CT scans of sheep knees and used to produce CAD moulds that were 3D printed out of acrylonitrile butadiene styrene (ABS) plastic. Alginate-cell solution was cross-linked with CaSO<sub>4</sub> and cultured for up to 8 weeks *in vitro*. Anatomical shape was retained and constructs had both mechanical and biochemical properties similar to that of native tissues [9] (Fig. 2A). Future efforts are now focusing on stimulating extracellular matrix (ECM) production as well as evaluation of geometric fidelity based on imaging type and time in culture.

### Rapid prototyping

Rapid prototyping has many different variations (Table 2). The basis for this technique is to produce usable scaffolds in a short

**Fig. 2** (A) An injection moulded menisci derived from a  $\mu$ CT scan and fibrochondrocyte seeded alginate after 8 weeks of *in vitro* culture [9]. (B) Medical grade PCL composite formed *via* fused deposition modelling (Image provided by Dr. Dietmar Hutmacher, Queensland University of Technology, AU). (C) Chondrocyte seeded alginate micro-channel network with  $50 \times 50 \mu\text{m}$  channels spaced  $100 \mu\text{m}$  apart [45]. (D) Cartilagenous disc 1 cm in diameter composed of PLG micro-beads seeded with chondrocytes after 8 weeks of *in vitro* culture [50].

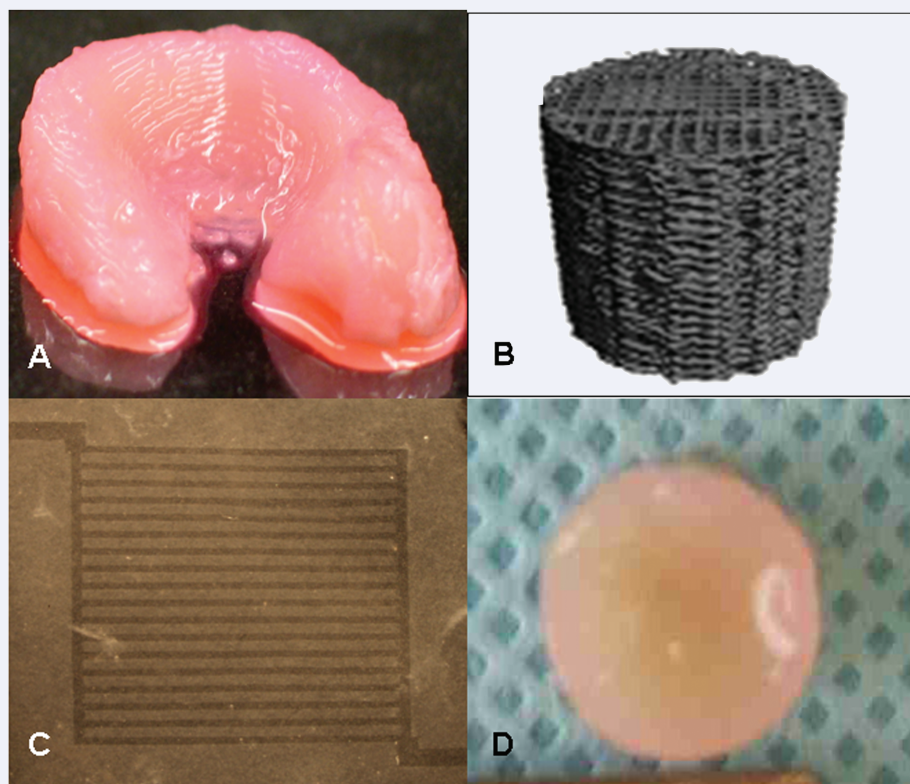


**Table 2** Fabrication techniques and the various biomaterials used for cell seeded scaffolds and acellular scaffolds as well as multi-cell/material capability and current resolution capabilities

Fabrication techniques	Variations	Seeded biomaterials	Non-seeded biomaterials	Multi-material/ multi-cell capable	Resolution
Moulding	Injection moulding	Alginate	PCL	No	600 $\mu\text{m}$
	Electro spun moulding	Agarose	PGA		
		Chitosan	PLA		
		Collagen			
		Fibrin glue			
Rapid prototyping	SFF	Alginate	PEG	Yes (but not CNC milling)	250 $\mu\text{m}$
	3D printing	Agarose	Porous coral		
	CNC milling	Chitosan	'TCP		
		Collagen	Tetracalcium phosphate		
Lithography	N/A	Alginate	Silicon	Yes	25 $\mu\text{m}$
		PEG	PEG		
		Collagen	PLG		
		Matrigel	PVA		
		Agarose	Collagen		
Sintering	N/A	PLG	PLG	No	40–600 $\mu\text{m}$
			PVA		
			HA		
			TCP		

time scale (*i.e.* hours to days). Solid freeform fabrication (SFF) and 3D printing are two of the more popular rapid prototyping techniques that are capable of generating multi-material and multi-cellular anatomical constructs. Hutmacher and Cool have nicely reviewed applications of SFF on bone tissue engineering in this journal [26] (Fig. 2B).

Most bone TE methods involve seeding of acellular constructs or insertion of acellular implants with the expectation of cellular ingrowth *in vivo*. Some successful studies include the use of porous coral in the shape of a distal phalanx seeded with periosteal cells for thumb reconstruction [8], 3D printing brushite implants [27] and a cranial segment [28] using tricalcium phosphate (TCP) and tetracalcium phosphate respectively. Shek *et al.* used localized gene therapy to increase and localize cellular and tissue ingrowth using an SFF polypropylene fumarate/TCP composite that provided a stable matrix that could be matched to specific patient defect geometry [29]. Work by Sherwood *et al.* in conjunction with Therics, Inc. (Princeton, NJ, USA) produced osteochondral composites using TCP combined with either PLG or PLA for the chondral surface [30]. The composite structure exhibited region specific mechanical properties and integration between the two biomaterials making it suitable for implantation [30]. Therics, Inc. also has a number of other TCP based therapeutic products that are currently undergoing clinical studies. SFF techniques are able to produce patient specific scaffolds that can be modified to increase and guide cellular in growth through variation of surface roughness, chemically bonded growth factors, and altered scaffold porosity [26].

For more heterogeneous tissues, such as the meniscus, heart valve and liver, control over spatial and temporal differences in cell type/morphology and mechanical properties is necessary. Achieving structures that have the necessary cell distributions and biomechanical properties is a major challenge. Cytoscribing, as termed by Klebe involved alternating deposition of layers of cells and materials to generate 2D and 3D tissues [31]. Klebe established this technique using a variety of different cell types from different species and bound them to substrates using fibronectin that was deposited *via* Hewlett Packard graphics plotter of ink jet printer [31]. More recently several groups have demonstrated simultaneous co-deposition of cells and materials. An excellent example of this is by Cohen *et al.* *via* SFF using alginate and chondrocytes [32]. The work established the ability to print cell seeded alginate using different materials (*i.e.* two different grades of alginate) and in different structurally sound shapes including a disc, crescent and meniscus based on  $\mu$ CT data with printing resolution of 270  $\mu$ m [32] (Table 2). Rapid prototyping has also been used in the fabrication of 3D hepatic tissues with complex internal microstructure. Constructs were generated using both multi-cell and multi-material as means to improve nutrient transport [33]. Cell printing efforts by Chang *et al.* have evaluated cell viability of HepG2 cells based on dispensing pressure and nozzle diameter with calcium cross-linked alginate [34] and combined these SFF techniques with lithography methods to generate 3D microorgans [35]. The microorgans had vascular networks serving as pharmacokinetic models and were able to replicate consistent prints with 250  $\mu$ m resolution [35] (Table 2).

## Lithography

The transport of solutes and removal of waste products is a large concern in TE, especially when trying to engineer large volume tissues or engineering organs like the liver. In the body this solute transport is accomplished primarily by the vascular system, which is effectively a network of perfused micro channels. Traditionally, engineered scaffolds have relied on the host to provide vascularization [36]. Lithography techniques have been applied to tissue engineering to produce predefined vasculature. Preliminary studies using a polydimethylsioxane (PDMS) substrate established the efficacy of this technique using both hepatocytes and endothelial cells [36]. Other biomaterials used in lithography TE efforts include polyvinyl alcohol (PVA) with fibroblasts [37], PCL and PLG with vascular smooth muscle cells [38], PEG with osteoblasts [39] and embryonic stem cells [40], matrigel with epithelial [41] cells and fibroblasts [42], as well as collagen and agarose with fibroblasts [42]. Other work done by Khademhosseini *et al.* generated 3D micropatterned substrates consisting of hyaluronic acid and fibronectin seeded with cardiomyocytes, which aligned along the interface between the scaffold and glass substrate [43].

Recent innovative studies using chondrocytes seeded in alginate have shown great promise in their ability to generate various microfluidic patterns *via* laminated sheets with sealed channels as small as  $25 \times 25 \mu$ m [44, 45] (Table 2). After 4 weeks in culture, laminated sheets integrated well with no visible interface where two sheets were bonded together [46] (Fig. 2C). This work by Choi and coworkers really demonstrates the resolution of image based TE and can be implemented to produce larger volume constructs that not only have a custom circulation network, but a network that can be controlled spatially with gradients of nutrients, growth factors and region-specific flow rates [44–46].

## Sintering

The deposition of micro-particles or micro-beads to alter surface properties or to build up structures is known as sintering. Sintering has become a valuable fabrication technique that allows designation of specific localized properties that control for porosity, surface chemistry and mechanical properties. Most sintering efforts have focused on its application to bone TE through the use of PVA [47], hydroxyapatite (HA) [47], TCP [48] and PLG [49]. Studies have shown improved osteoblast cell growth throughout the sintered matrix [49].

Other works done with PLG and its application to cartilage tissue engineering have shown its ability to be used as a mouldable scaffold [50] capable of cellular proliferation and infiltration *in vivo* [51] (Fig. 2D). The use of sintering cell seeded PLG micro-beads in combination with free chondrocytes can be used to address focal defects *in vivo*. Furthermore, integrating the use of image guided tissue engineering bead-cell mixtures can be deposited to repair articular surfaces to their original geometry before injury. The repair resolution of this technique is only limited by the consistency and size of the micro particles/bead, which can range from 40–600  $\mu$ m [47–51] (Table 2).

## Conclusions

Image guided tissue engineering shows great promise for the generation of patient specific engineered tissues. CT and MRI can provide adequate templates for custom, patient-specific implants. Other imaging modalities do hold promise but have yet to be established. Although most image based efforts have focused on musculoskeletal tissues, image-based templates are starting to be used for cardiovascular models and small scale micro-vascular channels for hepatic tissues *via* CAD. The methods for generating these constructs vary greatly depending on the scale, tissue type and biomaterial. There exists the possibility to not only generate constructs that mimic the gross anatomy, but also generate proper substructure and networks of the desired tissue.

Both injection moulding and SFF techniques can generate anatomically shaped TE constructs that appear to have high geometric fidelity. A major challenge to all who work on image-guided tissue engineering lies in the lack of methods to quantify shape fidelity of fabricated implants. Similarly, there is essentially no data describing how shape fidelity is maintained throughout culture whether *in vivo* or *in vitro*. These issues are complicated by the fact that there is still no established technique for evaluating shape fidelity of anatomically shaped TE constructs. The topic of shape fidelity is still in dire need of further investigation, because for many of these complex shaped tissues such as the meniscus [52–54] or heart valve [55, 56] critical dimensions and tolerance levels for implantation are still being debated.

It is clear that medical imaging is an excellent tool to quantitatively define the geometry of structures especially *in situ*, such as the meniscus or heart valve. Now with new advances in medical imaging techniques, location specific microstructure can be extracted as well. Three-dimensional printing can provide the ability to create tissue-specific properties that vary with location within the tissue/organ (*i.e.* cell type, mechanical properties, porosity, etc.), which would otherwise not be possible with injection moulding. Spatial properties can be gathered from medical images to aid in the construction of engineered tissues. MRI [57] and  $\mu$ CT [58] have been used to look at GAG concentration in cartilage, CT to look at bone density and trabecular architecture [59], second harmonic generation microscopy to look at collagen fibre orientation [60] and density [61]. Combining imaging data techniques with rapid prototyping could allow generation of anatomical structures *in situ* with region specific microstructure similar to that of native tissues.

## References

1. **Vacanti CA.** The history of tissue engineering. *JCMM*. 2006; 10: 569–76.
2. **Saleh K, Olson M, Resig S, et al.** Predictors of wound infection in hip and knee joint replacement: results from a 20 year surveillance program. *J Orthop Res*. 2002; 20: 506–15.
3. **Miller CM, Gondolesi GE, Florman S et al.** One hundred nine living donor liver transplants in adults and children: a single-center experience. *Annals Surg*. 2001; 234: 301–11.
4. **Lietz K, John R, Mancini DM, et al.** Outcomes in cardiac transplant recipients using allografts from older donors versus mortality on the transplant waiting list; Implications for donor selection criteria. *J Am Coll Cardiol*. 2004; 43: 1553–61.
5. **Menick FJ.** Facial reconstruction with local and distant tissue: the interface of aesthetic

Imaging tools and fabrication techniques have enhanced fabrication of engineered constructs, but on the list of tissue engineering goals this seems to be only the tip of the iceberg. How exactly does one go from a newly fabricated construct and produce engineered tissues ready for implantation? Even without considering shape fidelity, quality control for TE implants involves confirming that these tissues have the appropriate biochemical composition and mechanical function. For dynamically loaded tissues such as the heart valve or meniscus, complicated geometry often results in complicated mechanics. For years, medical imaging has been used to extract geometries of bones, muscles, and cartilage to develop constitutive models to better describe the inner workings of joints in the body through finite element modelling (FEM). Medical imaging combined with FEM will continue to play a major role in assessing the functionality and durability of engineered tissues. As new knowledge is acquired about *in vivo* behaviour through FEM simulations, engineered tissues can be specifically conditioned *in vitro* to withstand these stresses.

The idea of *in vitro* conditioning is becoming more and more popular not only for engineered tissues such as tendon [62], heart valve [63], bone [64] and cartilage [65], but for cadaveric explants as well [65, 66]. Exposure to limited *in vivo* like stimuli in a reduced or gradual manner has shown to be beneficial to cells and resulted in increased ECM formation as well as corresponding improvements in mechanical behaviour. Optimal *in vitro* conditioning settings have yet to be elucidated, but as it stands now the time scale for generating functional tissues is lengthy.

Nonetheless image-guided tissue engineering is still likely a very valuable tool for generating patient specific tissues and organs. Challenges still lie in the ability to integrate these techniques to engineer large volume tissues with micro-vasculature and generate proper ECM organization and alignment. These techniques in combination with *in vitro* conditioning will enable the generation of spatially complex and more functional tissues.

## Acknowledgements

The authors would like to thank the following people and funding sources for their contributions to this work: Timothy M Wright, Suzanne A Maher, Hollis G Potter, Alfred P. Sloan Fellowship, MRRCC Core grant: AR046121 and Cornell University.

- and reconstructive surgery. *Plast Reconstr Surg.* 1998; 102: 1424–33.
6. **Cao Y, Vacanti JP, Paige KT, et al.** Transplantation of chondrocytes utilizing a polymer-cell construct to produce tissue-engineered cartilage in the shape of a human ear. *Plast Reconstr Surg.* 1997; 100: 297–302.
  7. **Weng Y, Cao Y, Silva CA, et al.** Tissue-engineered composites of bone and cartilage for mandible condylar reconstruction. *J Oral Maxillofac Surg.* 2001; 59: 185–90.
  8. **Vacanti CA, Bonassar LJ, Vacanti MP et al.** Replacement of an avulsed phalanx with tissue-engineered bone. *N Eng J Med.* 2001; 344: 1511–4.
  9. **Ballyns JJ, Gleghorn JP, Niebrzydowski V, et al.** Image-guided tissue engineering of anatomically shaped implants via MRI and micro-CT using injection molding. *Tissue Eng A.* 2008; 14: 1195–202.
  10. **Theysohn JM, Maderwald S, Kraff O, et al.** Subjective acceptance of 7 Tesla MRI for human imaging. *Magma NY.* 2008; 21: 63–72.
  11. **White D, Chelule KL, Seethom BB.** Accuracy of MRI vs CT imaging with particular reference to patient specific templates for total knee replacement surgery. *Int J Med Robot.* 2008; 4: 224–31.
  12. **Elliott MR, Thrush AJ.** Measurement of resolution in intravascular ultrasound images. *Physiol Meas.* 1996; 17: 259–65.
  13. **Verhey JF, Nathan NS, Rienhoff O, et al.** Finite-element-method (FEM) model generation of time-resolved 3D echocardiographic geometry data for mitral-valve volumetry. *Biomed Eng Online.* 2006; 5: 17.
  14. **Little SH, Igo SR, McCulloch M, et al.** Three-dimensional ultrasound imaging model of mitral valve regurgitation: design and evaluation. *Ultrasound Med Biol.* 2008; 34: 647–54.
  15. **Chang SC, Rowley JA, Tobias G, et al.** Injection molding of chondrocyte/alginate constructs in the shape of facial implants. *J Biomed Mater Res.* 2001; 55: 503–11.
  16. **Isogai N, Landis W, Kim TH, et al.** Formation of phalanges and small joints by tissue-engineering. *J Bone Joint Surg.* 1999; 81: 306–16.
  17. **Kim WS, Vacanti JP, Cima L, et al.** Cartilage engineered in predetermined shapes employing cell transplantation on synthetic biodegradable polymers. *Plast Reconstr Surg.* 1994; 94: 233–7.
  18. **Chang SC, Tobias G, Roy AK, et al.** Tissue engineering of autologous cartilage for craniofacial reconstruction by injection molding. *Plast Reconstr Surg.* 2003; 112: 793–9.
  19. **Del Gaudio C, Bianco A, Grigioni M.** Electrospun bioresorbable trileaflet heart valve prosthesis for tissue engineering: *in vitro* functional assessment of a pulmonary cardiac valve design. *Ann Ist Super Sanita.* 2008; 44: 178–86.
  20. **Hott ME, Megerian CA, Beane R, et al.** Fabrication of tissue engineered tympanic membrane patches using computer-aided design and injection molding. *Laryngoscope.* 2004; 114: 1290–5.
  21. **Neidert MR, Tranquillo RT.** Tissue-engineered valves with commissural alignment. *Tissue Eng.* 2006; 12: 891–903.
  22. **Lee KW, Wang S, Lu L, et al.** Fabrication and characterization of poly(propylene fumarate) scaffolds with controlled pore structures using 3-dimensional printing and injection molding. *Tissue Eng.* 2006; 12: 2801–11.
  23. **Hung CT, Lima EG, Mauck RL, et al.** Anatomically shaped osteochondral constructs for articular cartilage repair. *J Biomech.* 2003; 36: 1853–64.
  24. **Mizuno H, Roy AK, Vacanti CA, et al.** Tissue-engineered composites of anulus fibrosus and nucleus pulposus for intervertebral disc replacement. *Spine.* 2004; 29: 1290–7.
  25. **Mizuno H, Roy AK, Zaporozhan V, et al.** Biomechanical and biochemical characterization of composite tissue-engineered intervertebral discs. *Biomaterials.* 2006; 27: 362–70.
  26. **Hutmacher DW, Cool S.** Concepts of scaffold-based tissue engineering—the rationale to use solid free-form fabrication techniques. *JCMM.* 2007; 11: 654–69.
  27. **Habibovic P, Gbureck U, Doillon CJ, et al.** Osteoconduction and osteoinduction of low-temperature 3D printed bioceramic implants. *Biomaterials.* 2008; 29: 944–53.
  28. **Khalyfa A, Vogt S, Weisser J, et al.** Development of a new calcium phosphate powder-binder system for the 3D printing of patient specific implants. *J Mater Sci.* 2007; 18: 909–16.
  29. **Schek RM, Taboas JM, Hollister SJ, et al.** Tissue engineering osteochondral implants for temporomandibular joint repair. *Orthod Craniofac Res.* 2005; 8: 313–9.
  30. **Sherwood JK, Riley SL, Palazzolo R, et al.** A three-dimensional osteochondral composite scaffold for articular cartilage repair. *Biomaterials.* 2002; 23: 4739–51.
  31. **Klebe RJ.** Cytoscribing: a method for micropositioning cells and the construction of two- and three-dimensional synthetic tissues. *Exp Cell Res.* 1988; 179: 362–73.
  32. **Cohen DL, Malone E, Lipson H, et al.** Direct freeform fabrication of seeded hydrogels in arbitrary geometries. *Tissue Eng.* 2006; 12: 1325–35.
  33. **Liu Tsang V, Chen AA, Cho LM, et al.** Fabrication of 3D hepatic tissues by additive photopatterning of cellular hydrogels. *FASEB J.* 2007; 21: 790–801.
  34. **Chang R, Nam J, Sun W.** Effects of dispensing pressure and nozzle diameter on cell survival from solid freeform fabrication-based direct cell writing. *Tissue Eng A.* 2008; 14: 41–8.
  35. **Chang R, Nam J, Sun W.** Direct cell writing of 3D microorgan for *in vitro* pharmacokinetic model. *Tissue Eng C Methods.* 2008; 14: 157–66.
  36. **Kaihara S, Borenstein J, Koka R, et al.** Silicon micromachining to tissue engineer branched vascular channels for liver fabrication. *Tissue Eng.* 2000; 6: 105–17.
  37. **Cheng CM, LeDuc PR.** Micropatterning polyvinyl alcohol as a biomimetic material through soft lithography with cell culture. *Molecular Biosyst.* 2006; 2: 299–303.
  38. **Sarkar S, Lee GY, Wong JY, et al.** Development and characterization of a porous micro-patterned scaffold for vascular tissue engineering applications. *Biomaterials.* 2006; 27: 4775–82.
  39. **Subramani K, Birch MA.** Fabrication of poly(ethylene glycol) hydrogel micropatterns with osteoinductive growth factors and evaluation of the effects on osteoblast activity and function. *Biomed Mater.* 2006; 1: 144–54.
  40. **Karp JM, Yeh J, Eng G, et al.** Controlling size, shape and homogeneity of embryoid bodies using poly(ethylene glycol) microwells. *Lab Chip.* 2007; 7: 786–94.
  41. **Sodunke TR, Turner KK, Caldwell SA et al.** Micropatterns of Matrigel for three-dimensional epithelial cultures. *Biomaterials.* 2007; 28: 4006–16.
  42. **McGuigan AP, Bruzewicz DA, Glavan A et al.** Cell encapsulation in sub-mm sized gel modules using replica molding. *PLoS ONE.* 2008; 3: e2258.
  43. **Khademhosseini A, Eng G, Yeh J, et al.** Microfluidic patterning for fabrication of contractile cardiac organoids. *Biomedical Microdevices.* 2007; 9: 149–57.
  44. **Cabodi M, Choi NW, Gleghorn JP, et al.** A microfluidic biomaterial. *J Am Chem Soc.* 2005; 127: 13788–9.
  45. **Choi NW, Cabodi M, Held B, et al.** Microfluidic scaffolds for tissue engineering. *Nature Mater.* 2007; 6: 908–15.



46. Lee CS, Gleghorn JP, Won Choi N, *et al.* Integration of layered chondrocyte-seeded alginate hydrogel scaffolds. *Biomaterials*. 2007; 28: 2987–93.
47. Wiria FE, Chua CK, Leong KF, *et al.* Improved biocomposite development of poly(vinyl alcohol) and hydroxyapatite for tissue engineering scaffold fabrication using selective laser sintering. *J Mater Sci*. 2008; 19: 989–96.
48. Tanimoto Y, Nishiyama N. Preparation and physical properties of tricalcium phosphate laminates for bone-tissue engineering. *J Biomed Mater Res A*. 2008; 85: 427–33.
49. Borden M, Attawia M, Laurencin CT. The sintered microsphere matrix for bone tissue engineering: *in vitro* osteoconductivity studies. *J Biomed Mater Res*. 2002; 61: 421–9.
50. Mercier NR, Costantino HR, Tracy MA, *et al.* Poly(lactide-co-glycolide) microspheres as a moldable scaffold for cartilage tissue engineering. *Biomaterials*. 2005; 26: 1945–52.
51. Mercier NR, Costantino HR, Tracy MA, *et al.* A novel injectable approach for cartilage formation *in vivo* using PLG microspheres. *Ann Biomed Eng*. 2004; 32: 418–29.
52. Dienst M, Greis PE, Ellis BJ, *et al.* Effect of lateral meniscal allograft sizing on contact mechanics of the lateral tibial plateau: an experimental study in human cadaveric knee joints. *Am J Sports Med*. 2007; 35: 34–42.
53. Huang A, Hull ML, Howell SM, *et al.* Identification of cross-sectional parameters of lateral meniscal allografts that predict tibial contact pressure in human cadaveric knees. *J Biomech Eng*. 2002; 124: 481–9.
54. Donahue TL, Hull ML, Howell SM. New algorithm for selecting meniscal allografts that best match the size and shape of the damaged meniscus. *J Orthop Res*. 2006; 24: 1535–43.
55. Rankin JS, Dalley AF, Crooke PS, *et al.* A 'hemispherical' model of aortic valvar geometry. *J Heart Valve Dis*. 2008; 17: 179–86.
56. Haj-Ali R, Dasi LP, Kim HS, *et al.* Structural simulations of prosthetic tri-leaflet aortic heart valves. *J Biomech*. 2008; 41: 1510–9.
57. Gray ML, Burstein D, Kim YJ, *et al.* 2007 Elizabeth Winston Lanier Award Winner. Magnetic resonance imaging of cartilage glycosaminoglycan: basic principles, imaging technique, and clinical applications. *J Orthop Res*. 2008; 26: 281–91.
58. Palmer AW, Goldberg RE, Levenston ME. Analysis of cartilage matrix fixed charge density and three-dimensional morphology via contrast-enhanced microcomputed tomography. *Proc Natl Acad Sci USA*. 2006; 103: 19255–60.
59. Fritton JC, Myers ER, Wright TM, *et al.* Bone mass is preserved and cancellous architecture altered due to cyclic loading of the mouse tibia after orchidectomy. *J Bone Miner Res*. 2008; 23: 663–71.
60. Yasui T, Tohno Y, Araki T. Determination of collagen fiber orientation in human tissue by use of polarization measurement of molecular second-harmonic-generation light. *Appl Opt*. 2004; 43: 2861–7.
61. Raub CB, Suresh V, Krasieva T, *et al.* Noninvasive assessment of collagen gel microstructure and mechanics using multiphoton microscopy. *Biophys J*. 2007; 92: 2212–22.
62. Androjna C, Spragg RK, Derwin KA. Mechanical conditioning of cell-seeded small intestine submucosa: a potential tissue-engineering strategy for tendon repair. *Tissue Eng*. 2007; 13: 233–43.
63. Flanagan TC, Cornelissen C, Koch S *et al.* The *in vitro* development of autologous fibrin-based tissue-engineered heart valves through optimised dynamic conditioning. *Biomaterials*. 2007; 28: 3388–97.
64. Wood MA, Yang Y, Thomas PB, *et al.* Using dihydropyridine-release strategies to enhance load effects in engineered human bone constructs. *Tissue Eng*. 2006; 12: 2489–97.
65. Schumann D, Kujat R, Nerlich M, *et al.* Mechanobiological conditioning of stem cells for cartilage tissue engineering. *Biomed Mater Eng*. 2006; 16: S37–52.
66. Shin SJ, Fermor B, Weinberg JB, *et al.* Regulation of matrix turnover in meniscal explants: role of mechanical stress, interleukin-1, and nitric oxide. *J Appl Physiol*. 2003; 95: 308–13.